

Opacitization Conditions of Hornblende in Bezmyannyi Volcano Andesites (March 30, 1956 Eruption)

P. Yu. Plechov^a, A. E. Tsai^a, V. D. Shcherbakov^a, and O. V. Dirksen^b

^a *Geological Faculty, Moscow State University, Vorob'evy Gory, Moscow, 119899 Russia*
e-mail: pavel@web.ru

^b *Institute of Volcanic Geology and Geochemistry, Far East Division, Russian Academy of Sciences, bul'v. Piipa 9, Petropavlosk-Kamchatskii, 683006 Russia*

Received May 24, 2006

Accepted after revision November 11, 2006

Abstract—The paper is devoted to the conditions under which opacite rims developed around hornblende grains in andesite of the catastrophic eruption (March 30, 1956) of Bezmyannyi volcano, Kamchatka. The opacite rims were produced by a bimetasomatic reaction between hornblende and melt with the development of the following zoning: hornblende $\rightarrow Px + Pl + Ti-Mag \rightarrow Px + Pl \rightarrow Px \rightarrow$ melt. Bimetasomatic reaction was accompanied by the active removal of CaO from the rim, addition of SiO₂, and more complicated behavior of other components. The hornblende also shows reactions of its volumetric decomposition under near-isochemical conditions. The opacite rims developed under isobaric conditions, at a pressure of approximately 6 kbar. The main reason for the instability of the hornblende was the heating of the magma chamber from 890 to 1005°C due to new hot magma portion injection. The time interval between the injection and the start of eruption was estimated from the thickness of the opacite rims and did not exceed 37 days. Hence, the March 30, 1956, eruption was not related to the volcanic activity in November of 1955 but to the injection of a fresh magma portion in February–March of 1956.

DOI: 10.1134/S0869591108010025

INTRODUCTION

Bezmyannyi volcano (55.98°N, 160.58°E, height 2880 m a.s.l.) is the only active andesite volcano in the Klyuchevskoi group (Fig. 1). Its catastrophic eruption on March 30, 1956, and the ensuing period of activa-

tion, which continues for more than 50 years, make this volcano one of the world's most active volcanoes. However, the March 30, 1956, catastrophic eruption was preceded by a few episodes of eruptive activity that started on October 22, 1955. The dynamics of magma



Fig. 1. Bezmyannyi volcano. August 2005.

ascent immediately before the catastrophic eruption is of undisputable interest. The key problems there are as follows: (1) what was the immediate cause of this catastrophic eruption, and (2) whether the eruption episodes at Bezymyanni in 1955–1956 were genetically related or they were independent episodes that took place at an overall resumption of the volcanic activity.

A clue for understanding the dynamics of magma ascent is provided by studying uncompleted mineral reactions. The andesites of Bezymyanni volcano contain hornblende with opacite rims. These rims are opaque (in transmitted light) rims of mafic minerals in volcanic rocks and are reaction products of these minerals with the ambient melt. The opaqueness of opacite rims is largely caused by their significant contents of ore minerals (titanomagnetite or magnetite and ilmenite). The term *opacite* was coined by Vogelsang (1867) to denote an unidentifiable mineral that was found by this researcher in the form of “black opaque blebs”. Levinson-Lessing (1933) published micrographs of opacite rims around hornblende grains in andesites from the Central Caucasus and refers to the experiments of Kuzu and Yoshiki (1927) that demonstrated the possibility of hornblende decomposition during heating.

The causes and mechanisms of the development of opacite rims remain uncertain as of yet and were actively discussed for many years in the literature (see, for example, Levinson-Lessing, 1933; Lodochnikov, 1955; Garcia and Jacobson, 1979; Rutherford and Hill, 1993; Rutherford and Devine, 2003; Buckley et al., 2006). The instability of hornblende and its decomposition can be triggered by several factors, for example, melt degassing during its decompression (Kuno, 1950; Garcia and Jacobson, 1979; Rutherford and Devine, 2003; Buckley et al., 2006), a temperature increase (Rutherford and Devine, 2003), and/or oxidation of the melt (Garcia and Jacobson, 1979; Murphy et al., 2000; Rutherford and Devine, 2003).

Many researchers mention that the same samples may contain various types of reaction rims around hornblende and absolutely fresh and unaltered hornblende grains, which possibly suggests the simultaneous action of various factors that destabilized this mineral. Garcia and Jacobson (1979) distinguished two types of reaction rims: (1) a black type, in which amphibole is completely or partly replaced by fine-grained aggregates of Fe oxides and pyroxene and (2) a gabbroic type, in which amphibole is completely or partly replaced by fine- to medium-grained aggregates of orthopyroxene, clinopyroxene, plagioclase, and magnetite. These authors arrived at the conclusion that the gabbroic type develops in response to a decrease in water fugacity in the magmatic reservoir, whereas the black type results from the oxidation during eruption. Murphy et al. (2000) distinguished three types of reaction rims around amphibole in eruption products of Soufriere Hills volcano: (1) fine-grained (5–30 μm)

aggregates of mutually intergrowing clinopyroxene, orthopyroxene, pigeonite, plagioclase, and titanomagnetite, which develop in the form of rims and along cleavage planes in crystals; (2) coarser grained (30–200 μm) aggregates of the same phases as in type 1; and (3) opaque (true opacite) replacing aggregates that both formed rims and developed along cleavage in many minerals. Opacite aggregates are, according to these researchers, made up of extremely fine-grained intergrowths (1–10 μm) of the same phases as in types 1 and 2 but with titanomagnetite dominating over other mafic minerals. Murphy et al. (2000) believe that type 1 is produced in the course of amphibole dehydration during magma ascent, type 2 reflects a long-lasting recrystallization history, and type 3 corresponds to the latest oxidation stage in the extrusion dome. Rutherford and Devine (2003) mention that the same rock may sometimes contain more than one population of hornblende with different types of reaction rims. The eruption products of Soufriere Hills volcano contain, according to these authors, (1) thin (1–20 μm) rims that developed during decompression in the course of magma ascent; (2) much thicker (200–500 μm) coarse-grained clinopyroxene-dominated rims produced by thermal decomposition; and (3) aggregates of ore minerals along cleavage and other cracks, which were formed due to oxidation (Rutherford and Devine, 2003).

In a series of their experimental studies, Rutherford and Hill (1993) have demonstrated experimentally that reaction rims can be utilized to evaluate the time during which the hornblende reacted with the ambient melt (Rutherford and Hill, 1993) or to assay the ascent velocity of the magmas (see, for example, Rutherford and Devine, 2003). Reaction rims are formed during reactions with melt (Rutherford and Hill, 1993) and are controlled by diffusion processes (Coombs and Gardner, 2004). Many researchers (Rutherford and Hill, 1993; Rutherford and Devine, 2003; Buckley et al., 2006) identify a repose time period during which no rims replaced the hornblende. This publication deals with some issues concerning the types of the decomposition reactions of hornblende in products of the March 30, 1956, eruption of Bezymyanni volcano and the mechanisms that could form these rims. Based on isobaric experiments on hornblende decomposition (Rutherford and Hill, 1993; Rutherford and Devine, 2003) and petrographic observations, we consider the process forming the rims as controlled by a bimetasomatic reaction with melt and propose an equation for estimating the time during which this reaction proceeded. Our temperature and time estimates obtained for the reaction rims provide insight into processes that occurred in the magma chamber immediately before the catastrophic eruption on March 30, 1956.

METHODS

All analyses of minerals and glasses were accomplished on a Cameca SX100 (Hobart Uni, Australia)

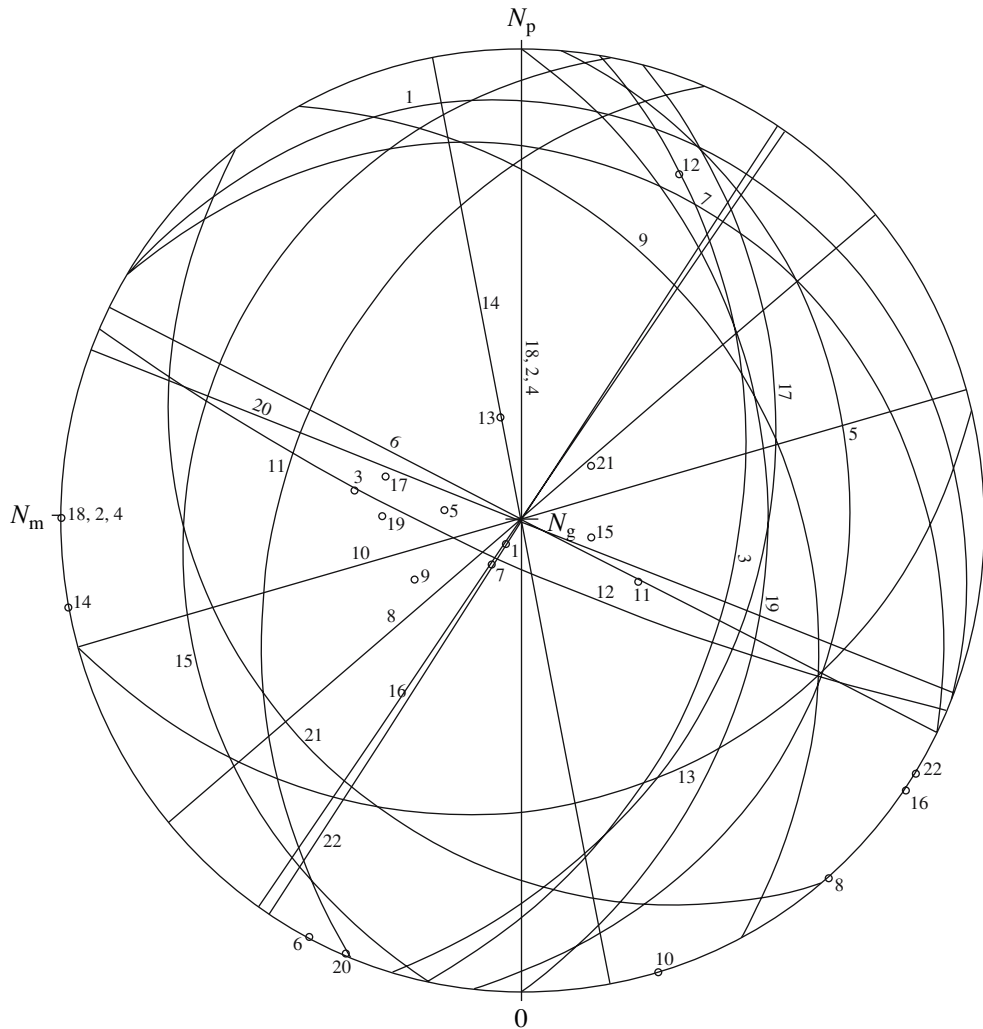


Fig. 2. Section planes of hornblende grains in a spherical projection (Wulff net). Points show perpendiculars to the examined sections, numerals nearby are their numbers.

microprobe at an accelerating voltage of 15 kV and a current of 20 nA. The beam diameter was 5 μm . Backscattered electron (BSE) images were taken on a Cam-Scan-4DV electron microscope at the Department of Petrology, Moscow State University, at an accelerating voltage of 20 kV.

The thicknesses of the reaction rims around hornblendes were measured in thin sections, in sections of hornblende grains whose orientation was determined on a Fedorov universal stage. For each grain, spherical coordinates were determined for at least two traces of its indicatrix axes. The third indicatrix axis was then constructed as a perpendicular to the former two. The indicatrix axes were identified using the Berek wedge compensator. The orientation of a given section plane was then calculated relative to the N_p and N_m axes (Fig. 2), which coincide for hornblende with its crystallographic X and Y axes, respectively (Tröger, 1956). For each section, the hkl coordinates were determined and the section "depth" and faces were identified for each

face of each section using the SHAPE computer program. For each face in each section, we conducted eight to ten measurements of the visible thicknesses of the rims at various sites at the face. The measurements were conducted in BSE images, because they exhibit only phases exposed at the surface of the sample section.

Table 1 presents the true thicknesses of the rims in each set of the measurements. The true thicknesses of the rims were calculated as a projection onto a perpendicular to a given crystal face. The measurements on the face (001) were conducted in maximally elongated grains, and other measurements were conducted in hexagonal sections of various orientation. The thicknesses of the rims on the face (001) were greater than on all other faces. However, as can be seen from Table 1, the difference is within the accuracy of the measurements.

In order to determine the mineral composition of the reaction rims, we selected their portions of two struc-

Table 1. Measured thicknesses of reaction rims in cross sections of certain orientation in hornblende grains

Grain no.	α , degree	(010), μm	(110), μm	($\bar{1}10$), μm	(001), μm	Average over grain, μm
1	5	20.90	18.85	20.07		19.58
2	90		29.05		18.61	23.83
3	49	17.06	19.86	18.46		18.58
4	90		29.02		23.51	26.27
5	26	24.26	26.60	33.31		27.93
6	90		24.00		30.00	27.00
7	12	25.24	22.77	26.14		24.44
8	90		24.00		32.00	28.00
9	35	23.13	22.65	22.41		22.67
10	74				23.04	23.04
11	31	32.87	31.85	30.23		31.16
12	85		24.00		26.91	25.46
13	20	19.65	23.37	21.97		21.96
14	90		24.00		24.00	24.00
15	25	31.51	37.16	22.85		29.83
16	90				24.00	24.00
17	38	23.73	20.48	23.20		21.86
18	90				30.00	30.00
19	44	22.43	25.36	20.51		22.65
20	76		24.00		29.12	26.56
21	25	27.26	25.17	22.71		24.32
22	81				29.66	29.66
Average		24.37	25.12	23.80	26.44	25.13
Standard deviation		4.75	4.42	4.45	4.09	3.40

Note: Grain numbers correspond to those in Fig. 2. α is the dihedral angle between a given section and the (001) plane. Each column summarizes measurements for two crystal faces (with direct and reverse indices). The last column reports averaged thicknesses for each grain.

tural types: granular and symplectitic. In each grain, we conducted measurements of two types: first we determined the mineralogical composition of the whole rim and then the composition only of its granular portion with regard for cavities. Phases were distinguished based on contrast in the BSE images and were transformed in four-color images with each color corresponding to a certain phase. The percentages of the phases were then calculated by counting pixels within the areas of the images corresponding to each phase.

1955–1956 ERUPTION OF BEZYMANNYI VOLCANO

The volcano started to develop in the Late Pleistocene and evolved in a number of stages: at 11 000–

7800 years BP, 5500–3300 years BP, 2400–1700 years BP, and 1350–1000 years BP (radiocarbon dating, Braitseva et al., 1990). The 1955–1956 eruption began unexpectedly, after a millenarian interlude in the eruptive activity of this volcano. Volcanic precursor events were noted to start half a year before the March 30, 1956, eruption and occurred in the following succession (Gorshkov and Bogoyavlenskaya, 1965):

* September 29, 1955—first seismic event, during which the number of seismic shocks and their intensity gradually increased. The original depths of the hypocenters was estimated at 50 km, the epicenters plotted in the area of Bezymyanniy volcano.

* October 22, 1955, 6 a.m.—first Vulcanian-type ash eruptions began simultaneously with unceasing seismic shocks. Ash falls occurred at the townships of Klyuchi and Ust'-Kamchatsk, and their intensity progressively increased and reached a maximum on November 16–17. Eruptive activity diminished by November 21. The amount of ash accumulated over one month at Klyuchi reached 22 mm (close to 15 kg/m²).

* The time period from late November of 1955 till March of 1956 was marked by insignificant eruptions not associated with ash falls.

* Gorshkov and Bogoyavlenskaya (1965) suggested that a lava dome grew in February–March of 1956 based on the fact that two or three lava blocks were identified within the pyroclastic material during an aircraft fly-out.

* March 28, 1956—after a two-month interlude, a very weak ash fall occurred at the township of Klyuchi, and March 30, 1956, was marked by a catastrophic eruption of Bezymyanniy volcano.

Thus, the activity of Bezymyanniy volcano before its eruption on March 30, 1956, included two episodes: the first lasted from October 22 through November 20, 1955, and the second began on March 28, 1956, i.e., only three days before the catastrophic eruption.

The directional explosion at the volcano on March 30, 1956, destroyed its summit and eastern slope (Gorshkov and Bogoyavlenskaya, 1965). The explosion broke, cut, and partly charred large trees within up to 25 km. The thickest ash deposits of this explosion accumulated within a narrow sector at the bottom of the volcano over an area of 60 km². The thickness of the pyroclastic deposits outside this sector (over an area of 500 km²) ranged from 1 m (near the volcano) to 1 cm. The flow expanded for 18 km along the valley of the Sukhaya Khapitsa River, and an eruption cloud 50 km in diameter rose to an altitude of 35–40 km. The volume of juvenile material exceeded 1 km³, and the total volume of displaced material amounted to 2.6–2.8 km³ (Bogoyavlenskaya et al., 1985).

Immediately after the March 30, 1956, eruption, a new extrusion dome started to grow in the newly formed crater.

SAMPLES

For our research, we selected two large volcanic bombs (Fig. 3) from the pyroclastic deposits of the March 30, 1956, eruption. The characteristic cracking of these bombs testifies that they were still hot when fell and cracked at the collision or immediately after it due to rapid cooling in air. The bombs had a relatively low porosity (~40%). These characteristics suggest that the bombs were fragments of a cryptodome, which was emplaced into the volcanic edifice immediately before the 1956 eruption and deformed its southeastern slope (Gorshkov and Bogoyavlenskaya, 1965). The samples were used to examine the textural and morphological characteristics of the opacite rims around hornblende and to determine the mineralogical composition of the rims and the conditions under which they developed.

PETROGRAPHY AND MINERALOGY OF PRODUCTS OF THE MARCH 30, 1956, ERUPTION

Products of the March 30, 1956, eruption consist of hornblende andesite with plagioclase, orthopyroxene, hornblende, and titanomagnetite in phenocrysts and plagioclase, orthopyroxene, titanomagnetite and minor amounts of glass in the groundmass. The petrography and petrochemistry of the eruption products were described in detail in (Gorshkov and Bogoyavlenskaya, 1965).

Megascopically, the rocks are pale gray, with clearly visible phenocrysts of pale plagioclase and dark hornblende, and have a porphyritic texture (20–25% phenocrysts). The predominant phenocrysts are plagioclase (60–65%) and hornblende (25–30%), and orthopyroxene phenocrysts are much more rare, with most of them occurring in cumulophyric aggregates with plagioclase. The rocks may contain rare titanomagnetite phenocrysts.

The juvenile material of the March 30, 1956, eruption is characterized by an almost unvarying chemical composition (Table 2; Gorshkov and Bogoyavlenskaya, 1965) and corresponds to andesite of the calc-alkaline series according to (Gill, 1981). The average compositions of minerals and glasses are presented in Table 2. The phenocryst plagioclase has weakly zonal cores (An_{50-55}) and clearly pronounced bimodal zoning in margins. The zoning consists of a resorption zone with numerous tunnel melt inclusions and consisting of An_{64-68} and an outer rim 10–30 μm thick of “pure” plagioclase around the resorption zone. The outer rim shows normal zoning from An_{62-64} to An_{54-55} . Plagioclase phenocrysts of analogous structure were described in many arc volcanics and were interpreted as testifying to the injection of hotter and CaO-rich magma into the chamber (see, for example, Tepley et al., 1999).

Hornblende phenocrysts are pleochroic in brown shades and have euhedral morphologies (Fig. 4). All

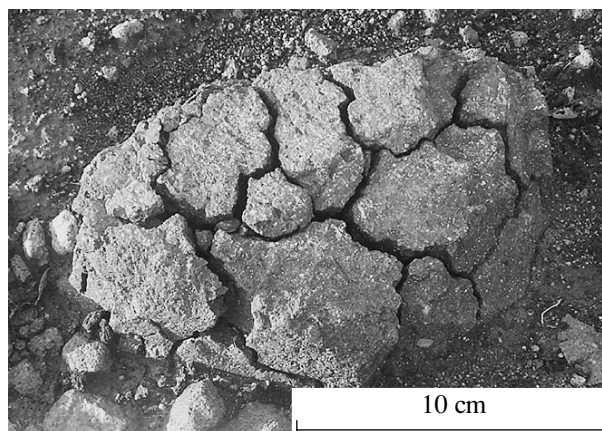


Fig. 3. Volcanic bomb with a breadcrust crack texture from the pyroclastic deposits of the March 30, 1956, eruption.

hornblende crystals are surrounded by reaction rims of roughly equal thickness (25–30 μm). Representative analyses of hornblende from our samples are listed in Table 3. In spite of the significant compositional variations, these phenocrysts show no clearly pronounced zoning. According to the systematics of (Leake et al., 1997), most of the hornblendes are magnesiohastingsite, although a few data points plotted within the fields of edenite and pargasite. The $\text{Fe}^{3+}/\text{Fe}^{2+}$ ratio in hornblende of Bezmyannyi volcano was evaluated by Mössbauer spectroscopy (Al'meev et al., 2002). The aforementioned authors believe that this ratio calculated from stoichiometric considerations (by normalizing to 13 cations) is systematically underestimated (due to underestimated Fe^{3+}). However, the occurrence of brown (basaltic) hornblende is thought to be related first of all to oxidation near the surface. This process is associated with the exsolution of minute magnetite lamellae (Murphy et al., 2000). The crystals examined by Al'meev et al. (2002) are secondarily oxidized brown hornblende, as follows from the presence of 18% magnetite found by these authors in the hornblende after separation. Thus, the $\text{Fe}^{3+}/\text{Fe}^{2+}$ ratios obtained by these authors in principle cannot reflect the primary Fe concentrations in hornblende from Bezmyannyi volcano during its crystallization and cannot be used to calculate the crystal chemical formulae of the hornblende.

The phenocryst orthopyroxene is pleochroic from greenish to pinkish color and occurs as euhedral equant or slightly elongated crystals with smooth reversed zoning and $\text{Mg}\# = \text{Mg}/(\text{Mg} + \text{Fe})$, at %, increasing from 65 in the cores of the phenocrysts to 67.5 in their outer zones. The $\text{Mg}\#$ of orthopyroxene microlites in the groundmass varies from 67.7 to 70.8. Clinopyroxene is rare in products of the March 30, 1956, eruption and is contained in them mostly as cumulophyric aggregates with orthopyroxene, plagioclase, and magnetite.

Table 2. Composition (wt %) of rocks and mineral phases in products of the March 30, 1956, eruption

Rock or mineral	SiO ₂	TiO ₂	Al ₂ O ₃	FeO	MnO	MgO	CaO	Na ₂ O	K ₂ O	P ₂ O ₅	Total
Rocks of the 1956 eruption (5)	60.06	0.76	17.55	6.20	0.15	3.19	6.82	3.53	1.39	–	99.65
Standard deviation	0.87	0.12	0.63	0.39	0.03	0.53	0.41	0.37	0.14	–	
Phenocrysts											
Plagioclase (72)	52.21	0.03	28.13	0.36	0.00	0.03	11.53	5.22	0.19	0.00	97.70
Standard deviation	1.48	0.02	1.00	0.08	–	0.02	0.94	0.71	0.12	–	
Magnetite (12)	0.07	7.52	1.91	79.95	0.59	1.19	0.00	0.00	0.00	0.00	91.25
Standard deviation	0.03	0.14	0.05	1.09	0.03	0.04	–	–	–	–	
Orthopyroxene (19)	52.28	0.14	0.73	20.70	1.14	23.02	0.85	0.00	0.00	0.00	98.86
Standard deviation	0.40	0.02	0.31	0.44	0.11	0.40	0.08	–	–	–	
Hornblende (43)	42.56	1.89	11.05	13.49	0.29	13.16	10.76	1.90	0.40	0.03	95.53
Standard deviation	1.06	0.34	1.52	1.19	0.08	0.65	0.82	0.24	0.07	0.01	
Groundmass											
Plagioclase (4)	52.41	0.00	28.68	0.60	0.02	0.05	11.72	4.47	0.31	0.03	98.29
Standard deviation	0.57	–	0.09	0.03	0.01	0.01	0.30	0.14	0.09	0.01	
Magnetite (5)	0.18	7.03	1.61	81.09	0.53	1.12	0.11	0.00	0.00	0.00	91.67
Standard deviation	0.03	1.21	0.50	0.99	0.05	0.10	0.04	–	–	–	
Orthopyroxene (5)	52.26	0.14	1.44	19.02	1.12	22.57	1.50	0.00	0.00	0.00	98.05
Standard deviation	0.45	0.02	0.31	1.20	0.04	1.12	0.15	–	–	–	
Glass (2)	76.70	0.37	11.37	1.41	0.04	0.09	0.33	2.43	5.19	0.04	97.98
Standard deviation	0.01	0.03	0.05	0.01	0.02	0.01	0.01	0.02	0.13	0.03	
Cristobalite (2)*	96.25	0.18	1.06	0.06	0.00	0.00	0.04	0.57	0.03	0.02	98.21
Standard deviation	0.51	0.01	0.05	0.03	–	–	0.02	0.08	0.01	0.01	
Melt inclusions											
In plagioclase**											
min***	56.3	0.58	17.76	4.91	0.08	1.73	6.45	4.56	4.9	0.28	97.78
max****	73.9	0.44	11.54	2.08	0.03	0.52	1.69	2.89	2.99	0.06	96.26
Mean (8)	67.41	0.39	16.03	2.12	0.06	0.91	3.59	3.97	4.17	0.12	98.87
Standard deviation	5.56	0.11	2.99	1.25	0.05	0.77	1.81	0.99	1.35	0.08	
In orthopyroxene											
Mean (8)	74.30	0.25	12.64	2.16	0.05	0.57	1.67	3.13	3.47	0.39	98.09
Standard deviation	2.05	0.19	1.01	0.52	0.04	0.73	1.65	1.80	1.37	0.56	

Note: Numerals in parentheses show the number of analyses. The compositions of rocks of the March 30, 1956, eruption are from (Malyshev, 2000). The analytical totals in (Malyshev, 2000) are normalized to 100 wt %, analytical total deviating from 100 wt % resulted from the recalculation of Fe to Fe²⁺.

* This phase was provisionally identified as cristobalite following the description in (Gorshkov and Bogoyavlenskaya, 1965). X-ray powder diffraction identification was not performed.

** Data from (Tolstykh et al., 1999) were used.

*** Melt inclusions with the lowest SiO₂ concentration.

**** Melt inclusions with the highest SiO₂ concentration.

Plagioclase phenocrysts contain crystalline inclusions of orthopyroxene and hornblende, and orthopyroxene and hornblende phenocrysts contain inclusions of plagioclase. This allowed us to recognize a simultaneously crystallizing phenocryst assemblage: plagioclase, orthopyroxene, and hornblende.

The composition of melt inclusions in the plagioclase reflect the broad major-component compositional variations of the melts. For example, the SiO₂ content varied from 56.3 to 73.9 wt %, and K₂O varied from 2.25 to 5.77 (Tolstykh et al., 1999). At the same time, melt inclusions in the orthopyroxene (Table 2) show

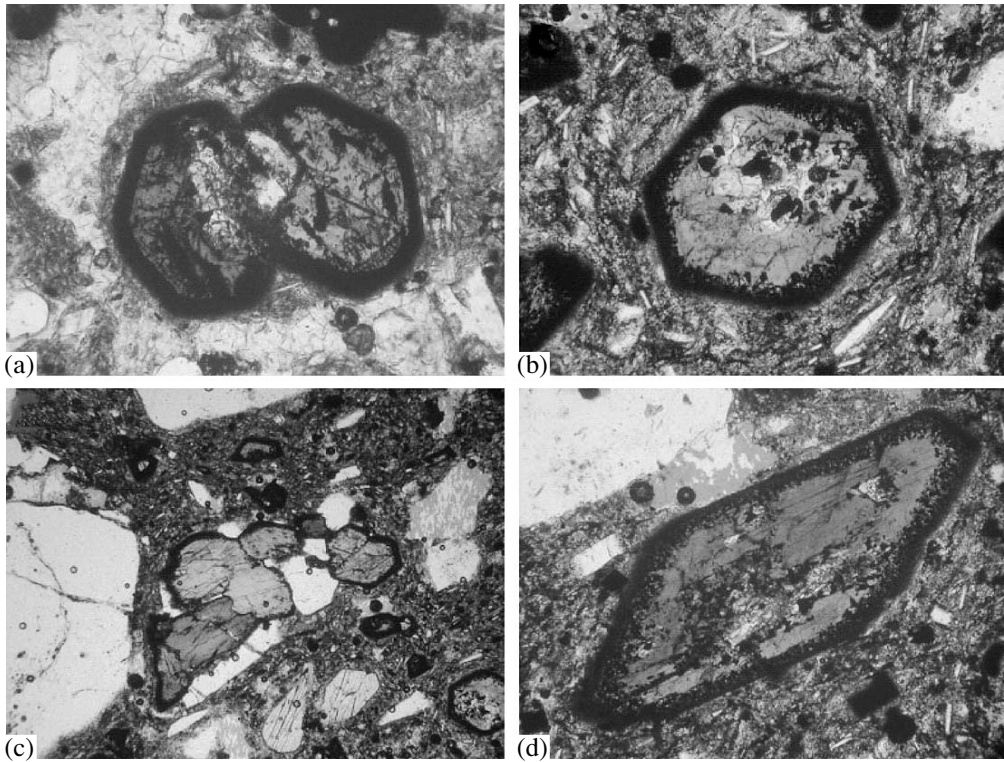


Fig. 4. Hornblende morphologies as seen in transmitted light.

- (a) Aggregate of two hornblende grains with opacite rims. The touching faces of the aggregate bear ingrowths of other minerals but no opacite rims.
- (b) Euhedral equant hornblende grain overgrown with an opacite rim of constant thickness and with a coarse-grained aggregate of volumetric hornblende decomposition (*Cpx-Opx-Pl-Mag*) inside.
- (c) Cluster of hornblende and plagioclase grains. Opacite rims developed only in contact of hornblende with the groundmass but not in contact with plagioclase.
- (d) Euhedral elongated hornblende grain with an opacite rim and domains of volumetric decomposition.
- The long side of each photo is equal to 0.8 mm.

much narrowed compositional variations: $\text{SiO}_2 = 72.5\text{--}74.0$ wt %, $\text{K}_2\text{O} = 2.35\text{--}3.27$ wt %. We did not find any melt inclusions in the hornblende. The compositional range of melts from which plagioclase could crystallize simultaneously with orthopyroxene corresponds to a silicity range of 72.3 to 73.9 wt %. Conceivably, the broader variations in the compositions of melt inclusions in the plagioclase testify that it crystallized from compositionally variable melts at their mixing front.

The groundmass is dominated by plagioclase and orthopyroxene microlites, whose proportion is hard to assay because of numerous relics of completely decomposed hornblende. The groundmass also contains many relatively large (up to 50–60 μm) fractured anhedral grains (Fig. 5), which were described by Gorshkov and Bogoyavlenskaya (1965) as cristobalite (~3%) and magnetite (<1%). The compositions of these phases are listed in Table 2. The cristobalite contains, along with SiO_2 , also Al_2O_3 and Na_2O . Rhyolitic glass occurs in the interstitial space between plagioclase crystals. Table 2 also lists the compositions of all groundmass phases.

Our samples are closely similar in mineralogy and petrography. Their differences in porosity can be explained by local processes and differences in the thermal history of the samples already during the eruption. The material of our samples is representative for studying processes that took place in the magma chamber before the March 30, 1956, eruption.

TYPES OF OPACITE RIMS

Andesites of the 1956 eruption of Bezmyannyi volcano contain hornblende surrounded by opacite rims visible in all cross sections of the crystals (Figs. 4–6). The hornblende crystals remain thereby euhedral: they usually display hexagonal cross sections with clearly pronounced crystal faces. Figures 6a–6c exhibit two textural types (granular and symplectitic) and their complicated relations. A granular rim (Fig. 6d) has sharp boundaries. On the hornblende side of this rim, it is most commonly bounded by a crack or cleavage plane. The morphology of the ore mineral can be equant or elongated, and its size varies from 3 to

Table 3. Composition (wt %) of hornblende phenocrysts

Analysis number	SiO ₂	TiO ₂	Al ₂ O ₃	FeO	MnO	MgO	CaO	Na ₂ O	K ₂ O	Total	Mg/(Mg + Fe)	Fe ²⁺ /Fe ³⁺	Al(IV)	Al(VI)	Total cations
1	42.85	1.54	9.57	13.91	0.34	13.37	10.49	2.07	0.44	94.57	0.84	0.51	1.61	0.08	15.36
2	43.69	1.60	9.34	13.20	0.31	13.91	10.70	1.63	0.43	94.81	0.87	0.40	1.54	0.09	15.24
3	43.60	1.92	9.38	14.16	0.35	13.46	10.54	1.56	0.42	95.38	0.86	0.38	1.58	0.05	15.19
4	45.18	1.65	8.37	12.72	0.26	13.82	10.63	2.25	0.50	95.38	0.77	1.35	1.31	0.15	15.43
5	43.70	1.95	8.64	13.73	0.28	13.63	10.63	1.56	0.43	94.54	0.84	0.52	1.50	0.02	15.23
6	41.49	1.74	9.65	14.02	0.32	12.55	10.61	1.65	0.42	92.44	0.80	0.64	1.64	0.10	15.31
7	42.69	1.58	9.52	13.91	0.40	13.95	11.02	1.50	0.34	94.91	0.90	0.26	1.66	0.00	15.24
8	43.16	1.73	9.77	14.09	0.34	13.17	10.62	1.68	0.44	95.00	0.83	0.49	1.60	0.11	15.25
9	41.51	1.58	11.10	15.35	0.44	12.52	10.24	2.15	0.41	95.29	0.86	0.32	1.84	0.10	15.32
10	42.03	1.58	10.83	15.60	0.48	12.59	10.36	1.89	0.39	95.76	0.86	0.29	1.80	0.08	15.25
11	43.76	2.12	9.24	14.51	0.32	14.03	10.39	2.16	0.36	96.89	0.88	0.31	1.58	0.00	15.29
12	43.61	2.05	9.98	12.97	0.25	14.11	10.72	1.79	0.54	96.02	0.87	0.40	1.63	0.09	15.29
13	43.92	1.96	10.36	12.22	0.22	14.54	10.77	1.83	0.51	96.34	0.90	0.33	1.63	0.14	15.28
14	40.75	1.97	12.95	12.04	0.21	13.20	10.50	2.17	0.38	94.16	0.89	0.33	1.94	0.33	15.37
15	41.41	1.91	13.68	11.88	0.22	13.50	10.92	2.21	0.35	96.08	0.88	0.36	1.97	0.38	15.39
16	42.63	1.49	12.67	11.86	0.22	13.73	10.70	2.03	0.31	95.63	0.90	0.30	1.79	0.38	15.30
17	42.85	1.71	13.20	13.24	0.21	13.58	10.83	2.13	0.36	98.12	0.89	0.28	1.89	0.33	15.31
18	42.04	1.69	12.12	13.96	0.27	12.63	10.75	1.96	0.38	95.80	0.82	0.52	1.81	0.29	15.33
19	42.12	2.16	11.76	13.82	0.26	12.70	10.72	2.01	0.47	96.02	0.81	0.63	1.80	0.24	15.35
20	44.15	1.91	10.01	12.18	0.31	14.50	10.64	1.81	0.47	95.96	0.90	0.32	1.58	0.13	15.25
21	43.92	1.77	10.17	13.17	0.32	13.46	11.16	1.82	0.50	96.29	0.79	0.92	1.55	0.20	15.37
22	42.95	1.88	10.97	14.37	0.27	12.71	10.65	1.94	0.45	96.20	0.80	0.64	1.69	0.21	15.31
23	42.74	1.94	11.57	14.31	0.27	12.65	10.84	1.90	0.44	96.65	0.80	0.65	1.75	0.25	15.32
24	41.74	1.91	11.45	14.04	0.27	12.38	10.65	1.88	0.42	94.75	0.80	0.65	1.77	0.24	15.33
25	42.54	1.87	11.62	14.25	0.29	12.90	10.80	1.87	0.42	96.56	0.83	0.47	1.79	0.21	15.30
26	42.17	2.00	12.02	15.15	0.26	12.50	10.55	1.77	0.41	96.82	0.85	0.35	1.86	0.20	15.22
27	43.20	2.10	12.54	13.00	0.18	11.82	10.62	1.97	0.46	95.88	0.72	1.61	1.63	0.55	15.33
28	42.19	2.05	12.62	14.05	0.25	12.44	11.06	2.09	0.41	97.16	0.78	0.81	1.85	0.32	15.40
29	41.92	1.99	12.91	13.47	0.21	12.62	10.96	2.08	0.40	96.57	0.80	0.69	1.87	0.36	15.38
30	41.88	1.99	13.12	13.27	0.24	12.80	11.12	2.02	0.41	96.84	0.82	0.63	1.90	0.36	15.38
31	41.60	1.91	13.12	13.34	0.21	12.71	10.95	2.02	0.40	96.26	0.83	0.56	1.91	0.36	15.37
32	42.30	1.64	9.84	14.50	0.43	13.65	10.77	1.67	0.38	95.18	0.90	0.23	1.71	0.00	15.26
33	41.49	1.63	9.45	13.90	0.43	13.25	10.42	1.68	0.37	92.61	0.89	0.28	1.69	0.00	15.26
34	41.35	1.46	9.46	14.21	0.48	13.41	10.56	1.68	0.38	93.00	0.90	0.22	1.69	0.00	15.28
35	42.27	2.83	10.91	13.77	0.26	12.98	10.83	1.86	0.41	96.12	0.81	0.66	1.78	0.11	15.32
36	41.66	3.01	10.78	15.85	0.29	12.86	10.16	2.11	0.39	97.10	0.87	0.27	1.85	0.00	15.25
37	42.00	2.03	12.57	12.93	0.22	13.24	10.66	2.11	0.33	96.09	0.87	0.38	1.87	0.29	15.33
38	41.46	1.99	12.50	12.94	0.19	13.10	10.71	2.12	0.31	95.32	0.86	0.42	1.89	0.28	15.35
39	41.39	2.06	12.62	13.00	0.22	13.05	10.55	2.19	0.32	95.39	0.87	0.38	1.91	0.28	15.35
40	41.30	2.12	12.81	13.17	0.22	12.75	10.79	2.25	0.33	95.73	0.82	0.60	1.91	0.31	15.41
41	42.79	2.69	10.80	13.81	0.30	13.06	10.70	1.77	0.40	96.32	0.82	0.56	1.74	0.13	15.26
Average	42.49	1.92	11.12	13.66	0.29	13.17	10.69	1.92	0.41	95.66	0.84	0.51	1.74	0.19	15.31
Standard deviation	0.98	0.33	1.48	0.94	0.08	0.61	0.22	0.21	0.05						
max*	45.18	3.01	13.68	15.85	0.48	14.54	11.16	2.25	0.54						
min**	40.75	1.46	8.37	11.86	0.18	11.82	10.16	1.50	0.31						

Note: Analyses 1–10 and 11–31 are microprobe profiles across hornblende grains; analyses 32–41 are individual hornblende grains. The hornblende formulae were calculated by normalizing to 13 cations.

* Maximum concentrations of major components in the measured hornblendes.

** Minimum concentrations of major components in the measured hornblendes.

8–10 μm . The plagioclase occurs as anhedral grains 5 to 10 μm across, and the predominant pyroxene is a matrix including ore minerals and plagioclase. The aggregate also contains minute cavities from 1.5 to 5 μm . The symplectitic rim (Fig. 6e) consists of fine (<1 μm) interlacing aggregates of minerals, whose composition cannot be determined even qualitatively. Judging from the contrast of the BSE images, the aggregates contain submicrometer-sized crystals of ore minerals.

Sections perpendicular to the elongation of the grains show both textural types of reaction rims: inner granular and outer symplectitic (Figs. 6a, 6b). The rims are characterized by a zonal distribution of the ore mineral: the outer rims exhibits a gradual decrease in the content of ore minerals from center to margin. In sections parallel to the elongation of hornblende crystals (Fig. 6c), it can be clearly seen that faces at the tops of the crystals are surrounded only by symplectite reaction rims, which also show a clearly zonal distribution of the ore mineral. Figure 6f displays a junction of top and side crystal faces of hornblende. The outer dark symplectitic rim surrounds both the side and top faces, and its thickness and composition do not vary. The granular rim, which is typical of the inner reaction zones of side faces, drastically gives way to a clearly pronounced symplectitic rim at faces at the top of the crystal. The boundaries of the rim remain sharp, and its thickness does not change. Reaction rims at side and top faces consist of two similar zones but differ in the morphology of grains in the inner zone.

Along with rims around crystals, the rocks contain coarse-grained (with grains up to 10–20 μm) aggregates of the decomposition products of hornblende inside its grains. This aggregate can touch the rim, cut across it, or be constrained within a hornblende grain and display no immediate contact with the rim (Fig. 7). Clinopyroxene in these domains inherits the orientation of the replaced hornblende. These aggregates have irregular morphologies or are equant, elongated, and are in places bounded by cleavage planes. Grains with these replacing aggregates are often cut by thin (a few micrometers) channels and fractures with acicular or platy ore minerals.

We recognized two major types of hornblende decomposition in andesites erupted in 1956 by Bezymyanni volcano. The first type comprises zonal opacite rims that surround hornblende grains and consist of two zones. This type, in turn, comprises two subtypes: of granular and symplectitic textures. The granular rims developed only on the side faces of hornblende crystals. The second type is the volumetric decomposition of hornblende. This type can also be subdivided into two subtypes. Coarse-grained replacement domains correspond to type 2 in (Murphy et al., 2000), the “gabbroic type” in (Garcia et al., 1979), and “clinopyroxene” type in (Rutherford and Devine, 2003). The fine-grained domains are the closest to the “black

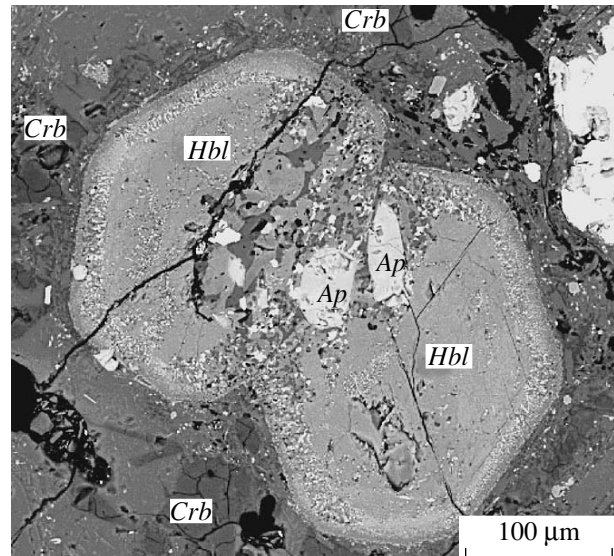


Fig. 5. BSE image of an aggregate of hornblende crystals in the groundmass. The image clearly shows numerous cristobalite grains and aggregates in the groundmass. The image shows the same site as in Fig. 4a (in which it is displayed in transmitted light). Mineral symbols: *Hbl*—hornblende, *Ap*—apatite, *Crb*—cristobalite.

type” in (Garcia et al., 1979), type 3 in (Murphy et al., 2000), and opacite in (Rutherford and Devine, 2003).

In spite of the seeming similarities of the hornblende replacement aggregates, due to certain reasons we cannot identify the opacitization rims with the products of the volumetric decomposition of hornblende. First, the chemical composition of the volumetric decomposition products is practically identical to the composition of the surrounding hornblende, whereas the opacite rims notably differ in composition from the hornblende (Table 4). Second, their mineralogical compositions are also different: the volumetric decomposition products contain Ca-rich clinopyroxene, while the granular aggregates of the opacite rims contain only orthopyroxene and pigeonite. Third, domains of volumetric decomposition cut across opacite rims, i.e., are younger than they (Fig. 7).

DECOMPOSITION REACTIONS OF HORNBLLENDE

Rutherford and Hill (Rutherford and Hill, 1993) note that the development of reaction rims around hornblende in the Sent Helens andesites requires the participation of melt because (i) reaction rims are absent from places shielded from the melt by other phases, and (ii) melt participation is evident from textural features of the growth of the rims inward the crystals. Opacite rims on hornblende in rocks of Bezymyanni volcano show analogous evidence of their interaction with the ambient melt (Fig. 4).

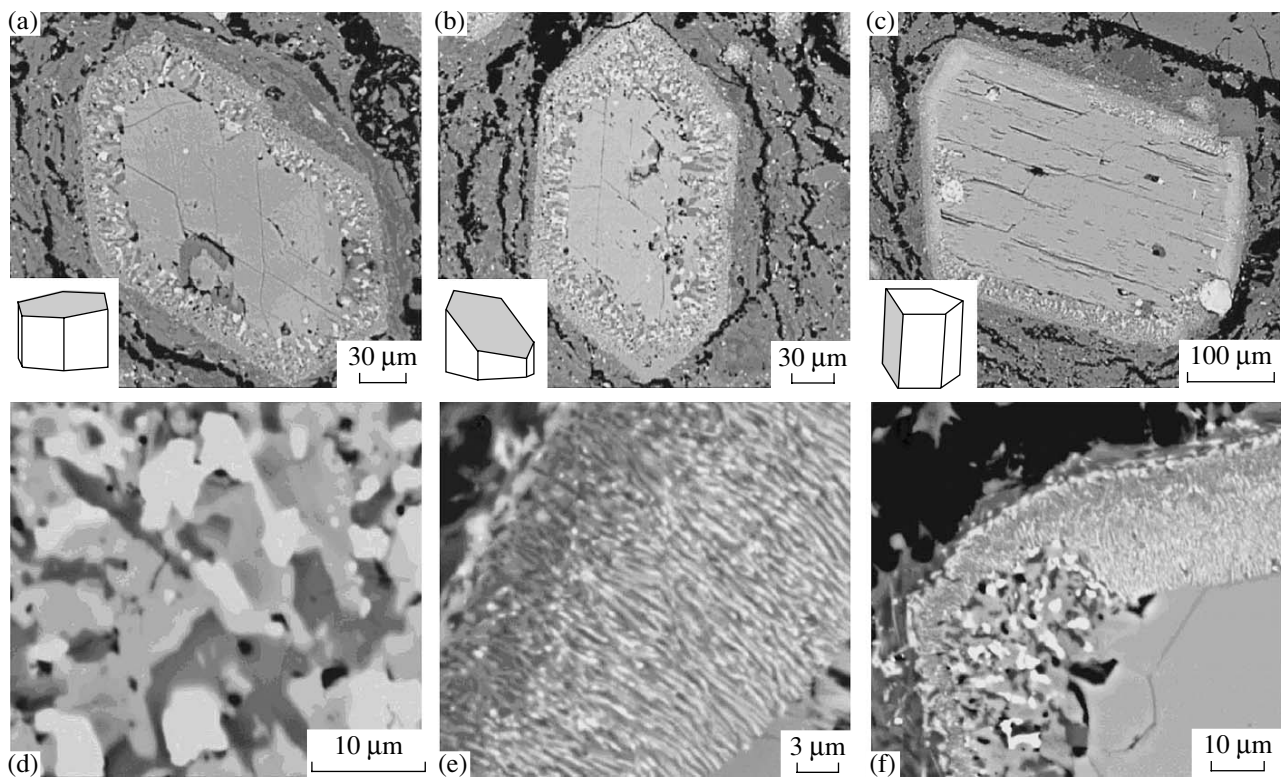


Fig. 6. (a–c) Various sections of hornblende grains and their crystallographic orientation. (d–f) Textural types of the rims. (a, b) Sections perpendicular to the hornblende crystal elongation; (c) section along crystal elongation; (d) granular type of rims; (e) symplectitic type of rims; (f) junction of faces at the top and side of hornblende crystals.

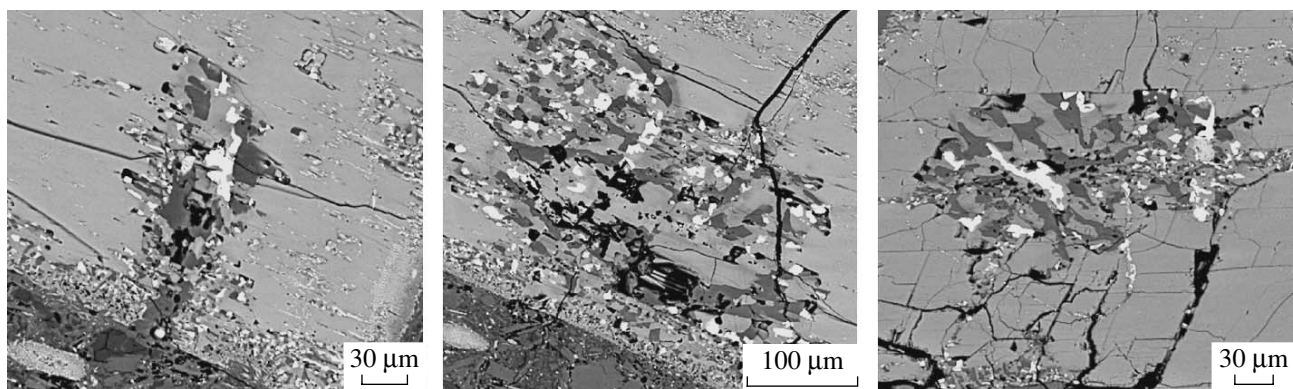


Fig. 7. Coarse-grained decomposition aggregate within a hornblende crystal.

Buckley et al. (2006) believe that the reaction of hornblende decomposition is nearly isochemical but proceeds in an open system, with an insignificant component exchange with the melt. The mass balance calculations are complicated by the zoning of the hornblende and the broad compositional variations of minerals in the reaction rims, i.e., the uncertainty in compositions of phases participating in the mass balance. Nevertheless, all cases analyzed by these authors

required SiO_2 introduction from the melt and the removal of FeO , CaO , and alkalis from the hornblende.

The decomposition reactions of hornblende reported in the literature are summarized in Table 5. Domains with the volumetric decomposition of hornblende in rocks from Bezmyannyi volcano can be realistically described by the isochemical reaction proposed in (Buckley et al., 2006). In these domains, pyroxene obviously dominates over other minerals, and plagioclase is contained in subordinate amounts (Fig. 7). The content

Table 4. Composition (wt %) of hornblende decomposition products

Minerals	SiO ₂	TiO ₂	Al ₂ O ₃	FeO	MnO	MgO	CaO	Na ₂ O	K ₂ O	P ₂ O ₅
In rim										
Plagioclase (4)	49.77	0.29	25.78	1.97	0.07	1.93	12.80	3.54	0.45	0.02
Standard deviation	1.01	0.26	2.29	1.06	0.03	1.14	0.34	0.33	0.13	0.01
Magnetite (2)	2.94	8.42	3.87	62.79	0.57	3.71	0.67	0.10	0.03	0.01
Standard deviation	3.95	1.57	0.83	10.01	0.11	0.88	0.54	0.12	0.00	0.01
Orthopyroxene (3)	52.28	0.14	0.73	20.70	1.14	23.02	0.85	0.00	0.02	0.01
Standard deviation	0.40	0.02	0.31	0.44	0.11	0.40	0.08	0.01	0.01	0.01
Outer rim (22)*	51.20	0.93	12.69	10.34	0.53	12.37	7.30	2.20	0.34	0.04
Standard deviation	2.35	0.54	2.53	1.52	0.16	2.11	2.50	0.41	0.37	0.02
Inner rim (41)*	43.72	2.01	10.25	16.36	0.49	12.16	10.31	1.53	0.18	0.03
Standard deviation	1.71	0.37	2.03	2.49	0.11	1.54	1.45	0.45	0.11	0.03
In domains of volumetric decomposition										
Plagioclase (5)	53.61	0.09	26.50	1.25	0.03	0.24	9.71	5.22	0.74	0.03
Standard deviation	2.20	0.05	0.89	0.30	0.02	0.15	0.56	0.10	0.15	0.01
Magnetite (4)	0.30	5.72	3.14	75.16	0.69	5.78	0.23	0.00	0.01	0.00
Standard deviation	0.41	3.15	0.51	3.05	0.01	1.62	0.12	0.01	0.01	0.00
Orthopyroxene (4)	53.00	0.37	1.68	14.92	0.69	26.19	1.88	0.03	0.01	0.01
Standard deviation	0.21	0.05	0.56	1.32	0.02	0.78	0.20	0.01	0.01	0.01
Clinopyroxene (10)	48.80	1.11	3.18	7.56	0.39	15.68	19.49	0.42	0.04	0.02
Standard deviation	2.56	0.22	0.67	1.26	0.06	1.46	1.44	0.11	0.06	0.02
Aggregate of volumetric hornblende decomposition (31)**										
	44.84	1.47	11.96	11.99	0.57	13.78	9.72	1.84	0.29	0.03

Notes: * Average compositions in profiles across certain portions of the rims.

** Average compositions in profiles across completely decomposed hornblende grains.

Table 5. Hornblende decomposition reactions reported in the literature

Reactants, wt %	Products, wt %	Reference, volcano
73 <i>Hbl</i> + 27 <i>Melt</i>	29 <i>Opx</i> + 24 <i>Cpx</i> + 43 <i>Pl</i> + 3 <i>Ilm</i>	(Rutherford and Hill, 1993), Sent Helens
100 <i>Hbl</i>	49.8 <i>Cpx</i> + 27.6 <i>Opx</i> + 18.2 <i>Pl</i> + 4.5 <i>Ti-Mag</i>	(Buckley et al., 2006), Montserrat
100 <i>Hbl</i>	53.9 <i>Cpx</i> + 24.4 <i>Opx</i> + 18.1 <i>Pl</i> + 1.9 <i>Ilm</i> + 1.7 <i>Mag</i>	(Buckley et al., 2006), Montserrat
100 <i>Hbl</i>	43.0 <i>Cpx</i> + 24.5 <i>Opx</i> + 23.7 <i>Pl</i> + 5.2 <i>Ilm</i> + 3.5 <i>Mag</i>	(Buckley et al., 2006), Sent Helens

of the ore mineral in these domains strongly varies but generally does not exceed 8 wt %. In our rocks, the only ore mineral is titanomagnetite (Table 4), although some rocks from Sent Helens (Buckley et al., 2006) and Montserrat (Murphy et al., 2000) volcanoes contain reaction rims with two ore minerals: magnetite and ilmenite.

Opacite rims on hornblende in rocks from Bezymannnyi volcano could not be formed by the reactions proposed in (Rutherford and Hill, 1993; Buckley et al., 2006) due to the following reasons:

(1) The opacite rims contain no Ca-rich clinopyroxene, which is the main mineral in the proposed reac-

tions. Pyroxene in the rims contains from 0.5 (orthopyroxene) to 12 wt % (pigeonite) CaO (Table 4). High-Ca clinopyroxene is contained only in the domains of volumetric hornblende decomposition, which developed after the opacite rims.

(2) The mineral proportions in the reaction rims principally differ from those in the proposed reactions. We measured the proportions of pyroxene, the ore mineral, and plagioclase in the rims as a whole and separately in their granular parts. The results of these measurements and recalculation into weight percentages are listed in Table 6. It can be seen that the granular rim is richer in the ore mineral than the outer symplectitic zones. Compared to the domains of volumetric decom-

Table 6. Measured mineral proportions in reaction rims and their recalculation into wt %

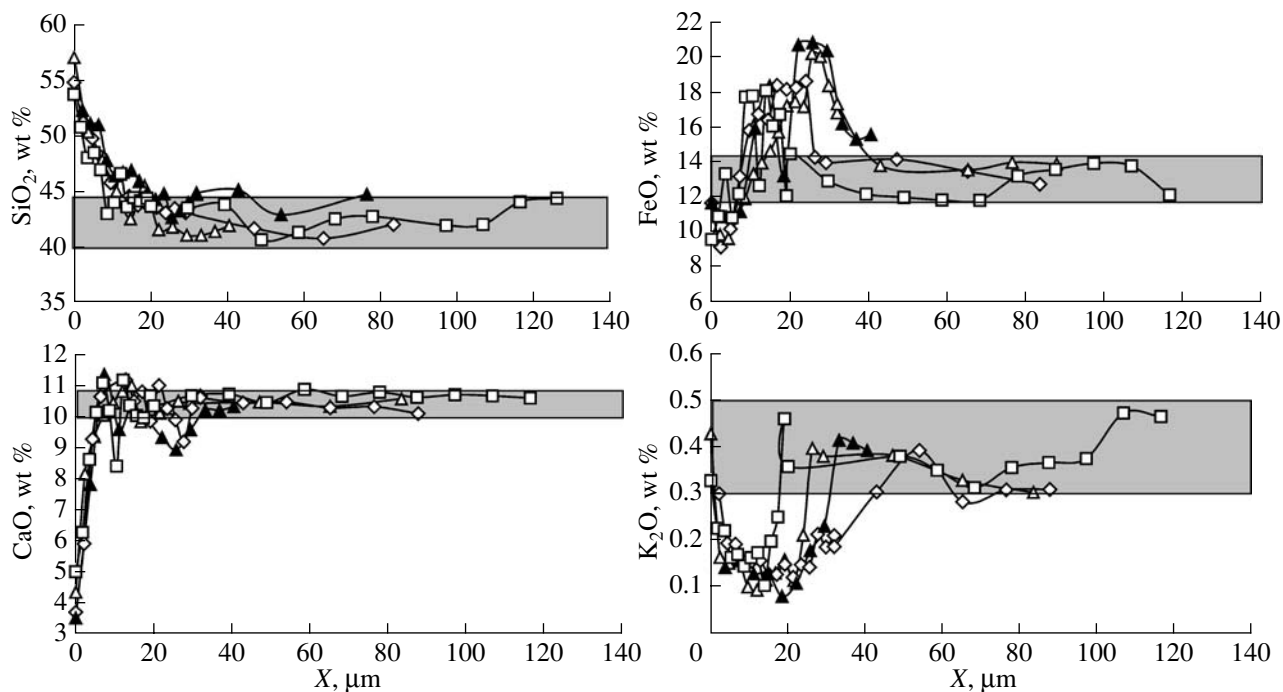
Grain no.	Granular parts of rims, vol %				Whole rim, vol %			Whole rim, wt %		
	<i>Px</i>	<i>Pl</i>	<i>Ti-Mag</i>	cavities	<i>Px</i>	<i>Pl</i>	<i>Ti-Mag</i>	<i>Px</i>	<i>Pl</i>	<i>Ti-Mag</i>
1	49.24	30.43	15.09	5.25	54.86	33.23	11.91	55.36	26.43	18.21
2	55.4	32.35	10.8	1.45	58.92	28.85	12.23	58.81	22.7	18.49
3	53.31	34.19	8.98	3.52	61.53	29.02	9.45	62.33	23.17	14.5
4	47.6	35.23	14.89	2.29	51.99	34.12	13.89	52.03	26.92	21.06
5	55.79	31.17	9.28	3.76	55.88	36.11	8.02	57.91	29.5	12.59
6	64.58	23.01	10.03	2.37	61.35	29.65	9	62.38	23.76	13.86
7	58.13	32.03	7.63	2.22	61.42	31.11	7.46	63.16	25.22	11.62
8	46.84	39.51	11.67	1.97	56.38	33.52	10.1	57.47	26.93	15.59
9	50.45	33.88	13.42	2.25	54.99	35.83	9.17	56.62	29.08	14.3
10	52.99	29.74	13.5	3.77	53.91	32.18	13.91	53.72	25.28	21
11	54.35	33.56	9.72	2.37	53.96	37.8	8.24	56.07	30.96	12.97
12	53.71	33.83	8.84	3.62	57.19	35.33	7.48	59.35	28.9	11.76
Mean	53.53	32.41	11.16	2.9	56.87	33.06	10.07	57.93	26.57	15.5
Standard deviation	4.87	3.91	2.52	1.08	3.26	2.96	2.35	3.49	2.66	3.39

position of hornblende and reactions proposed in (Buckley et al., 2006), opacite rims in rocks from Bezymyanni volcano contain much more ore mineral and plagioclase and much less pyroxenes.

(3) The rims of hornblende decomposition in rocks from Bezymyanni volcano display more clearly pronounced zoning, which is also pronounced in micro-

probe profiles across symplectite rims on faces at the tops of the crystals (Fig. 8).

This zoning can reflect the primary zoning of the hornblende crystals, i.e., the decomposition reaction could not be “almost isochemical”, contrary to what was proposed in (Buckley et al., 2006). Neither can the complicated and variably directed zoning be obtained by the simple addition of the composition of horn-

**Fig. 8.** Microprobe profiles across symplectitic rims. Gray fields show compositional variations of hornblende.

blende and a certain amount of melt, as was proposed in (Rutherford and Hill, 1993).

Complicated doubly directed processes of the selective removal and introduction of components are typical of bimetasomatic processes. A principally important distinctive feature of metasomatism is the development of metasomatic zoning, which is expressed in our samples in the presence of two zones: an inner zone of a three-phase assemblage (plagioclase + pyroxene + titanomagnetite) and an outer zone made up of a two-phase assemblage (plagioclase + pyroxene). On the side of melt, the hornblende is often overgrown by a micrometer-sized zone with pyroxene microlites. This zone can also be part of the metasomatic column. The zones distinguished in the metasomatic column at the boundary between melt and hornblende are shown in Fig. 9. Rare grains of an ore mineral in the *Px-Pl* zone are most probably relics of the *Px-Pl-Mag* zone. Thus, the bimetasomatic process of hornblende decomposition in andesite from Bezmyannyi volcano can be represented in the form of the following metasomatic column:

Hornblende	<i>Px + Pl + Ti-Mt</i>	<i>Px + Pl</i>	<i>Px</i>	Melt
------------	------------------------	----------------	-----------	------

SiO₂ migrates from the melt toward hornblende, and CaO is, conversely, removed from the hornblende. Other components behave in a more complicated manner and are redistributed between the zones of the metasomatic column (Fig. 8).

CONDITIONS INDUCING HORNBLLENDE DECOMPOSITION

Hornblende is a complex hydroxyl-bearing chain silicate, which is characterized by a limited stability field in magmatic rocks. Its crystallization requires a relatively high water partial pressure, a condition that makes hornblende unstable under pressures less than 1 kbar even in water-saturated systems. As was demonstrated experimentally, magma degassing due to decompression may destabilized amphiboles and their replacement by growing reaction rims (Rutherford and Hill, 1993).

The upper temperature stability limit of amphibole was thoroughly examined experimentally in various magmatic systems. Kadik et al. (1986) experimentally examined phase relations in andesites from Bezmyannyi volcano under various pressures and water concentrations and have demonstrated that the upper limit of hornblende stability does not exceed 950°C. Hence, system heating to higher temperatures should destabilized hornblende and result in its decomposition.

Some researchers (for example, Murphy et al., 2000) believe that opacitization reactions can proceed via hornblende oxidation during the growth of the extrusion dome. The stability limits of hornblende depending on f_{O_2} are known still relatively poorly. Scarce experiments (Barclay and Carmichael, 2004)

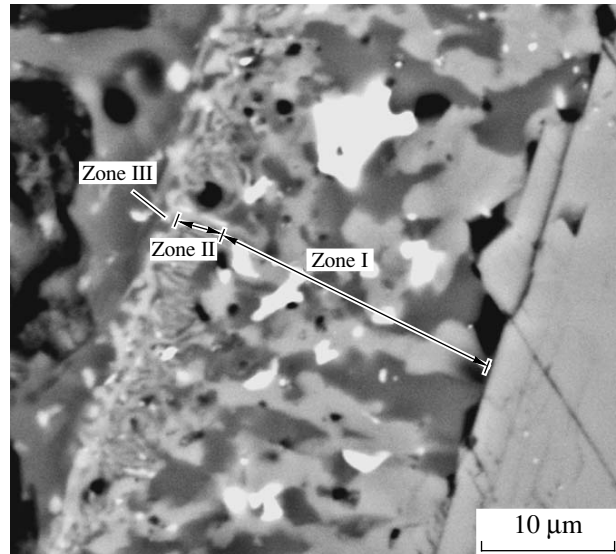


Fig. 9. Bimetasomatic zones in a rim. Zone I: *Px + Pl + Ti-Mag*; zone II: *Px + Pl*; zone III: *Px*.

have demonstrated that the stability field of hornblendes can expand to 1035°C at an increase in the oxygen fugacity to the $NNO + 2$ level in equilibrium with subalkaline basaltic andesite melt, which is, however, at variance with the traditional viewpoint concerning the development of opacite rims via melt oxidation and requires further experimental studying.

REASONS FOR HORNBLLENDE DECOMPOSITION IN ANDESITE FROM BEZMYANNYI VOLCANO

The crystallization conditions of phenocrysts in the hornblende andesite from Bezmyannyi volcano were estimated at 875–925°C, 3–8 kbar, and >6 wt % H₂O (Kadik et al., 1986). Al'meev et al. (2002) report a temperature range of 800–920°C and a pressure of approximately 6 kbar. A water content in the melts was also estimated at 3–4 wt % based on studying melt inclusions in the plagioclase (Tolstykh et al., 1999).

We determined the crystallization conditions of the phenocrysts by comparing the cotectic lines of acid melt (which were calculated by the MELTS computer program) with the results of plagioclase–hornblende thermometry (Holland and Blundy, 1994). The melt composition was assumed equal to the averaged composition of melt inclusions in the orthopyroxene (Table 2). Using the MELTS program (Ghiorso and Sack, 1995), we calculated a network of cotectic temperatures for various pressures and water concentrations. At a given water concentration and temperature, which was evaluated by (Holland and Blundy, 1994), we assayed the crystallization pressure. The minimum water concentration was assumed to be equal to 3 wt % (melt in the hornblende stability field). An increase in the specified

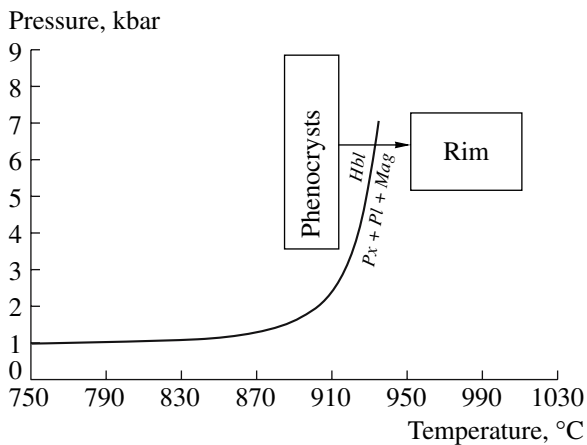


Fig. 10. Conditions under which hornblende grains could be opacitized in andesites erupted on March 30, 1956, by Bezymyanni volcano. Rectangles outline P - T regions in which the phenocrysts and rims were formed. The solid line shows the stability field of hornblende after (Rutherford and Hill, 1993).

water concentration by 0.5 wt % resulted (at the same pressure) to a decrease in the cotectic temperature for 15–20°C and a pressure overestimation by 1 kbar. In this method, the minimum pressure (5.1 kbar) can be obtained at the lowest water concentration (3 wt % H₂O). If the water content is assumed as was estimated in (Tolstyykh et al., 1999) for melt inclusions in plagioclase from rocks of the 1956 eruption (i.e., 3.5–4 wt % H₂O), then the crystallization temperature of the phenocrysts should be equal to $890 \pm 20^\circ\text{C}$ at a pressure of 6 ± 2 kbar. These values are in good agreement with literature data and lie within the stability field of hornblende (Kadik et al., 1986).

As was demonstrated above, the andesites of Bezymyanni volcano contain two types of hornblende decomposition: opacite rims and domains of volumetric decomposition. Two pyroxene–plagioclase–titano-magnetite mineral assemblages suitable for determining P - T conditions were found only in domains with volumetric hornblende decomposition. Opacite rims contain no clinopyroxene. The domains of volumetric hornblende decomposition cut opacite rims, but at the same time, the volumetric decomposition of hornblende was not completed and terminated at an early stage of this process. Thus, the temperatures and pressures at which the aggregates were formed during volumetric hornblende decomposition can be utilized as transitional conditions from the growth of the reaction rims around hornblende to the volumetric decomposition of this mineral. The temperatures at which the volumetric decomposition aggregates were produced was determined by two-pyroxene thermometers, by the method described in (Pletchov et al., 2005), and was $1005 \pm 36^\circ\text{C}$.

These temperatures determined for the decomposition of the hornblende are 100°C higher than the tem-

peratures at which the phenocryst assemblage crystallized. The heating could be induced by a newly arrived portions of hot and more basic magma. This idea receives support from the fact that the Mg# of orthopyroxene and the Ca# of the plagioclase increase in the marginal portions of the phenocrysts.

The pressure under which the volumetric decomposition aggregates developed was estimated by the techniques proposed in (Nimis and Ulmer, 1998). These authors made use of a correlation between the crystallization pressure and the unit cell volume of clinopyroxene, which was determined experimentally and in natural samples by single-crystal X-ray diffraction. Indeed, this phenomenon is the main factor affecting the unit cell volume of clinopyroxene, and its chemical composition is a dependent parameter, which is controlled by both the permissible unit cell volume and the composition of the melt. The practical application of this technique involves the evaluation of the structural parameters of the clinopyroxene unit cell from its composition and the subsequent evaluation of the crystallization pressure from the unit cell volume. The greatest uncertainty is related to the estimation of the unit cell volume, because clinopyroxene allows various schemes of isomorphism. Nimis with coworkers proposed a number of variants for the calibration for the estimates of the clinopyroxene unit cell parameters for basic magmatic systems. In our calculations, we made use of the calibration proposed for calc-alkaline melts (Nimis and Ulmer, 1998) as the most suitable for arc systems. The pressure values calculated for five clinopyroxene grains lie within a narrow range of 6.1–6.7 kbar, averaging at 6.4 kbar. Nimis and Ulmer (1998) reported the errors of this calibration as 1.7 kbar. The application of other proposed calibrations (Nimis and Ulmer, 1998) yielded pressures of no lower than 5 kbar. Thus, it is reasonable to think that a pressure of 6.4 ± 1.7 kbar in the magmatic system during hornblende decomposition corresponds (within the accuracy of the technique) to the crystallization pressure of the phenocryst assemblage, i.e., the decomposition of hornblende in andesite from Bezymyanni volcano occurred under isobaric conditions and was not related to the decompression of the magma and its degassing under pressures less than 1 kbar, as was proposed in (Rutherford and Hill, 1993) for Sent Helens volcano. The rapid oxidation of hornblende because of its contact with atmospheric oxygen also seems to have been hardly probable at depths of more than 20 km. Hence, the main reason for the decomposition of hornblende in andesite of Bezymyanni volcano was the isobaric heating of the magmatic chamber from 890 to 1005°C (Fig. 10).

THICKNESSES OF THE REACTION RIMS AND THEIR INTERPRETATION

The thicknesses of the reaction rims measured at hornblende grains of various orientation are summarized in Table 1. In spite of the differences in the mor-

phologies of the aggregates produced by the decomposition of hornblende along various crystallographic directions, the thicknesses of the rims are independent (within the error of the measurements) on the crystallographic direction in which the rims developed. The insignificant variations in the thicknesses of the rims on all of the examined grains suggest that the decomposition process was initiated practically simultaneously at all grains and did not depend on the location of the grains in the magmatic chamber.

The time during which the reaction rims developed was evaluated from the results of the experiments (Rutherford and Hill, 1993; Rutherford and Devine, 2003) (Fig. 11). The technique proposed in (Rutherford and Hill, 1993; Rutherford and Devine, 2003) is based on the results of decompression experiments modeling magma ascent during a certain eruption. As was demonstrated above, opacitization rims developed on hornblende in rocks of Bezmyannyi volcano under isobaric conditions. The factor controlling the growth rate of rims is the diffusion rate of components through the reaction rim (Coombs and Gardner, 2004). We use an equation similar to that of diffusion

$$t = t_0 + X^2/D, \quad (1)$$

where t is the time in days, X is the thickness of the rim in μm , t_0 is the repose time in days, and D is a coefficient. The least squares technique was used to treat the experimental results from (Rutherford and Hill, 1993; Rutherford and Devine, 2003) and determine the maximum range of D ($23.6\text{--}209.3 \mu\text{m}^2/\text{day}$, which corresponds to 2.7×10^{-16} to $2.0 \times 10^{-15} \text{m}^2/\text{s}$) and t_0 (2–5 days). The time required for the development the hornblende decomposition rims during the March 30, 1956, eruption of Bezmyannyi volcano and calculated using the maximum and minimum possible t_0 and D values was evaluated at 4–37 days.

INTERPRETATION OF VOLCANIC EVENTS THAT PRECEDED THE MARCH 30, 1956, ERUPTION

The time estimated for the development of reaction rims around hornblende grains in products of the March 30, 1956, eruption allowed us to revise the preexisting interpretations of the events preceding this eruption. The hot magma injection into the chamber that induced hornblende opacitization could take place in February or March of 1956, while the first eruptive activity of the volcano was identified on October 22, 1955, and a series of eruptions associated with ash falls continued only until late November. The mafic minerals in the ash of these eruptions are dominated by orthopyroxene (Gorshkov and Bogoyavlenskaya, 1965), and the products of the March 30, 1956, eruption are obviously characterized by hornblende predominance over orthopyroxene. Starting in November of 1955 until March of 1956, the magmatic chamber should have undergone significant transformations that induced a change in the

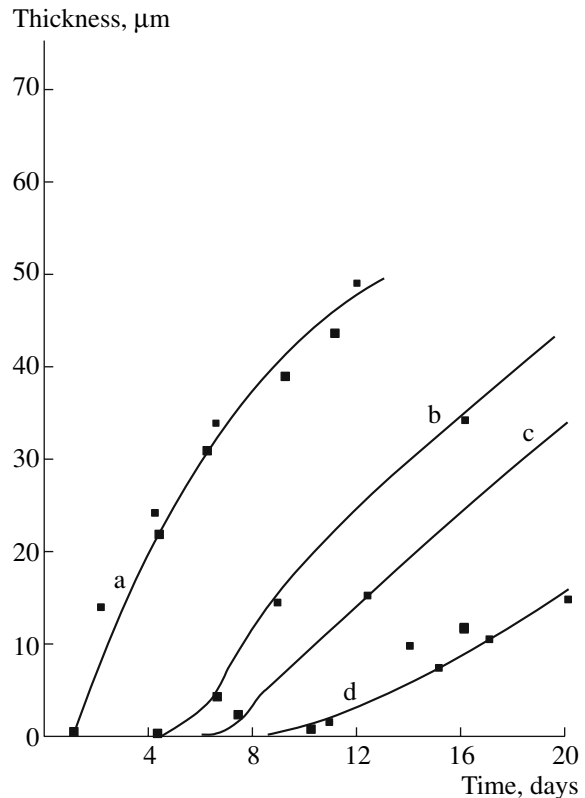


Fig. 11. Dependence of the thicknesses of the reaction rims on their growth time. Experimental conditions: (a) 900°C, 90 MPa; (b) 900°C, 160–2 MPa; (c) 900°C, 220–2 MPa; (d) 900°C, 20 MPa. The results of the experiments in (Rutherford and Hill, 1993; Rutherford and Devine, 2003).

phenocryst assemblage. Hence, the volcanic events in 1955 were not directly related to processes in the chamber before the March 30, 1956, eruption, but the magma portion involved in this eruption could have activate the long-lived chamber beneath Bezmyannyi volcano and cause the crystallization of hornblende phenocrysts. A fresh magma injection in February–March of 1956 caused the significant heating of the magmatic chamber, hornblende opacitization, growth of the outermost zones of the orthopyroxene and plagioclase phenocrysts with reversed zoning, and eventually, the catastrophic eruption on March 30, 1956.

CONCLUSIONS

1. The reactions of hornblende decomposition in andesites of the 1956 eruption of Bezmyannyi volcano can be subdivided into two major types: opacitization rims and reactions of volumetric decomposition.

2. The opacite rims developed because of a bimetasomatic reaction of the hornblende with melt with the origin of the following zoning: hornblende $\rightarrow Px + Pl + Ti\text{-}Mag \rightarrow Px + Pl \rightarrow Px \rightarrow$ melt. This reaction was associated with CaO removal from and SiO_2 introduction into the reaction rims with respect to the horn-

blende composition. Conversely, the reaction of volumetric hornblende decomposition was almost isochemical and resembles the reactions proposed in (Buckley et al., 2006).

3. The opacite rims developed under isobaric conditions. The main reason for hornblende instability was the heating of the magmatic chamber from 890 to 1005°C due to an injection of a fresh portion of hot magma.

4. The time elapsed from the hot magma injection into the chamber till the beginning of the eruption on March 30, 1956, was no longer than 4–37 days. The activity episode of Bezymyanni volcano in October–November of 1955 was not directly related to the March 30, 1956, catastrophic eruption.

ACKNOWLEDGMENTS

The authors thank L.V. Danyushevsky (University of Tasmania) for the provided possibility of detailed microprobe studies and fruitful discussion of the manuscript and G.I. Dorokhova (Moscow State University) for help in interpreting the crystallographic data. The authors also thank A.V. Giris (Institute of the Geology of Ore Deposits, Petrography, Mineralogy, and Geochemistry, Russian Academy of Sciences) for valuable and constructive criticism expressed during reviewing the manuscript. This study was supported by the program “Leading Scientific Schools in Russia” of the President of the Russian Federation (Grant 5338.2006.5, senior researcher L.L. Perchuk), a grant from the Royal Society, and the Russian Foundation for Basic Research (project no. 05-01-02901-YA-F_a).

REFERENCES

1. R. R. Al'meev, A. A. Ariskin, A. A. Ozerov, and N. N. Kononkova, “Problems of the Stoichiometry and Thermobarometry of Magmatic Amphiboles: An Example of Hornblende from the Andesites of Bezymyanni Volcano, Eastern Kamchatka,” *Geokhimiya*, No. 8, 803–819 (2002) [*Geochem. Int.* **40**, 723–738 (2002)].
2. J. Barclay and I. S. E. Carmichael, “A Hornblende Basalt from Western Mexico: Water-Saturated Phase Relations Constrain a Pressure-Temperature Window of Eruptibility,” *J. Petrol.* **45** (5), 485–506 (2004).
3. G. E. Bogoyavlenskaya, O. A. Braitseva, I. V. Melekestsev, et al., “Directed Explosion-Type Catastrophic Eruptions at the St. Helens, Bezymyanni, and Shiveluch Volcanoes,” *Vulkanol. Seismol.*, No. 2, 3–29 (1985).
4. O. A. Braitseva, I. V. Melekestsev, G. E. Bogoyavlenskaya, et al., “Bezymyanni Volcano: Evolution and Dynamics,” *Vulkanol. Seismol.*, No. 2, 3–22 (1990).
5. V. J. E. Buckley, R. S. J. Sparks, and B. J. Wood, “Hornblende Dehydration Reactions During Magma Ascent at Soufriere Hills Volcano, Montserrat,” *Contrib. Mineral. Petrol.* **151** (2), 121–140 (2006).
6. M. L. Coombs and J. E. Gardner, “Reaction Rim Growth on Olivine in Silicic Melts: Implications for Magma Mixing,” *Am. Mineral.* **89**, 748–759 (2004).
7. M. O. Garcia and S. S. Jacobson, “Crystal Clots, Amphibole Fractionation and the Evolution of Calc-Alkaline Magmas,” *Contrib. Mineral. Petrol.* **69**, 319–327 (1979).
8. M. S. Ghiorso and R. O. Sack, “Chemical Mass Transfer in Magmatic Processes. IV. A Revised and Internally Consistent Thermodynamic Model for the Interpolation and Extrapolation of Liquid–Solid Equilibria in Magmatic Systems at Elevated Temperatures and Pressures,” *Contrib. Mineral. Petrol.* **119**, 197–212 (1995).
9. J. Gill, *Orogenic Andesites and Plate Tectonics* (Springer, Berlin, 1981).
10. G. S. Gorshkov and G. E. Bogoyavlenskaya, *Bezymyanni Volcano and Its 1955–1963 Last Eruption* (Nauka, Moscow, 1965) [in Russian].
11. T. J. B. Holland and J. D. Blundy, “Non-Ideal Interactions in Calcic Amphiboles and Their Bearing on Amphibole–Plagioclase Thermometry,” *Contrib. Mineral. Petrol.* **116**, 433–447 (1994).
12. A. A. Kadik, A. P. Maksimov, and A. P. Ivanov, *Physicochemical Crystallization Conditions and Genesis of Andesites* (Nauka, Moscow, 1986) [in Russian].
13. Sh. Kozu and B. Yoshiki, “Die Dissoziationstemperatur von Brauner Hornblende und Ihre Rashe Expansion bei Dieser Temperatur,” *Sci. Rep. Tohoku Univ. Ser 3* (2), 7 (1927).
14. H. Kuno, “Geology of Hakone Volcano and Adjacent Areas, Japan,” *Geol. Soc. Am. Bull.* **61**, 957–1020 (1950).
15. B. E. Leake, A. R. Woolley, W. D. Birch, et al., “Nomenclature of Amphiboles: Report of the Subcommittee on Amphiboles of the International Mineralogical Association, Commission on New Minerals and Mineral Names,” *Can. Mineral.* **35** (1), 219–246 (1997).
16. F. Yu. Levinson-Lessing, *Petrography* (Gorgeonefteizdat, Leningrad–Moscow–Novosibirsk, 1933) [in Russian].
17. V. N. Lodochnikov, *Main Rock-Forming Minerals* (Gosgeoltekhizdat, Moscow, 1955) [in Russian].
18. A. I. Malyshev, *Life of the Volcano* (Ural. Otd. Ross. Akad. Nauk, Yekaterinburg, 2000) [in Russian].
19. M. D. Murphy, R. S. J. Sparks, J. Barclay, et al., “Remobilization of Andesite Magma by Intrusion of Mafic Magma at the Soufriere Hills Volcano, Montserrat, West Indies,” *J. Petrol.* **41** (1), 21–42 (2000).
20. P. Nimis and P. Ulmer, “Clinopyroxene Geobarometry of Magmatic Rocks. Part 1: An Expanded Structural Geobarometer for Anhydrous and Hydrous, Basic and Ultrabasic Systems,” *Contrib. Mineral. Petrol.* **133**, 122–135 (1998).
21. P. Yu. Pletchov, N. G. Zinovieva, N. P. Latyshev, and L. B. Granovsky, “Evaluation of the Crystallization Temperatures and Pressures for Clinopyroxene in the Parental Bodies of Ordinary Chondrites,” in *Proceedings*

- of 36th Lunar and Planetary Science Conference, Houston, USA, 2005* (Houston, 2005), No. 1041.
22. M. J. Rutherford and J. D. Devine, "Magmatic Conditions and Magma Ascent As Indicated by Hornblende Phase Equilibria and Reactions in the 1995–2002 Soufriere Hills Magma," *J. Petrol.* **44** (8), 1433–1454 (2003).
 23. M. J. Rutherford and P. M. Hill, "Magma Ascent Rates from Amphibole Breakdown: An Experimental Study Applied to the 1980–1986 Mount St. Helens Eruptions," *J. Geophys. Res.* **98**, 19667–19685 (1993).
 24. F. J. Tepley, J. P. Davidson, and M. A. Clynne, "Magmatic Interactions as Recorded in Plagioclase Phenocrysts of Chaos Crags, Lassen Volcanic Center, California," *J. Petrol.* **40**, 787–806 (1999).
 25. M. N. Tolstykh, V. B. Naumov, G. E. Bogoyavlenskaya, and N. N. Kononkova, "The Role of Andesitic–Dacitic–Rhyolitic Melts in the Crystallization of Phenocrysts in Andesite of Bezmyannyi Volcano, Kamchatka," *Geokhimiya*, No. 1, 14–24 (1999) [*Geochem. Int.* **37**, 1–10 (1999)].
 26. W. E. Tröger, *Optische Bestimmung der Gesteinsbildenden Minerale* (E. Schweizerbart'sche Verlagsbuchhandlung, Stuttgart, 1956; Gosgeoltekhizdat, Moscow, 1958) [in Russian].
 27. H. Vogelsang, *Philosophie der Geologie und Mikroskopische Gesteinsstudien* (Max Cohen & Sohn, Bonn, 1867).